Molecular Crystals and Liquid Crystals Incorporating Nonlinear Optics

Publication details, including instructions for authors and subscription information:
http://www.tandfonline.com/loi/gmcl17

Wave Structures in Nematic Layers

K. T. Schell [a] & R. S. Porter [a]

[a] Polymer Science and Engineering Department, University of Massachusetts, Amherst, Massachusetts, 01003

Version of record first published: 04 Oct 2006.

To cite this article: K. T. Schell & R. S. Porter (1989): Wave Structures in Nematic Layers, Molecular Crystals and Liquid Crystals Incorporating Nonlinear Optics, 174:1, 141-151

To link to this article: http://dx.doi.org/10.1080/00268948908042700

Mol. Cryst. Liq. Cryst., 1989, Vol. 174, pp. 141–151
Reprints available directly from the publisher
Photocopying permitted by license only

Printed in the United States of America

Wave Structures in Nematic Layers

K. T. SCHELL and R. S. PORTER

Polymer Science and Engineering Department, University of Massachusetts, Amherst, Massachusetts 01003

(*Received July 28, 1986; in final form, May 1, 1989*)

Wave structures have been observed in thin nematic layers of 4-4′-*n*-pentylcyanobiphenyl. This compound is nematic between 22 and 35°C. The wave structures are observed in transverse-field cells. In this geometry, the electric field (produced by an in-plane electrode structure) and the viewing direction are perpendicular. The wave structure occurs at the interface between electrically and surface oriented regions of the layer. Layer thickness was varied between 2.5 and 42 microns. The wavelength of the structure was found to vary from 15 to 280 microns depending on layer thickness and temperature. The conditions of voltage, frequency and temperature which promote the formation of the wave structure are discussed. The wave structure occurs in the dielectric regime of the electrical deformation.

INTRODUCTION

Mono-domains of nematic liquid crystals are readily deformed by electrical fields. The study of these deformations and resultant structures by optical methods fall within the field of electro-optics. In the past 20 years, many interesting effects, including dynamic scattering[1–2] and dielectric reorientation[3–5] phenomena, have been reported.

We wish to report here an interesting and reproducible wave structure found in electro-optical cells using a transverse-field geometry. Although this geometry (in which the electric field is produced by an in-plane electrode structure) has been used by previous researchers,[6–8] a detailed study of this structure is missing from the literature. The remarkable wave pattern studied here occurs at the interface between electrically and surface aligned molecules of a thin nematic layer. Establishing the stable wavelike interface depends on the conditions of field strength, frequency, temperature and layer thickness. Thus, we have undertaken a fundamental study of these conditions and explain the wave structure as a dielectric orientation pattern.

EXPERIMENTAL

The compound, 4-4′-*n*-pentylcyanobiphenyl (5CB), was chosen for study because of its large dielectric anisotropy ($\Delta\epsilon \approx 9$) and nematic state at ambient temperature.

These features facilitate dielectric reorientation of the molecules parallel to an applied field due to the highly polar cyano end group. This compound, as supplied by Merck, has a bulk ionic conductivity ($\sigma = 0.6 \times 10^{-10}$ nS/cm) and was used without further purification.

The nematic range for the commercial material as measured by DSC is given below:

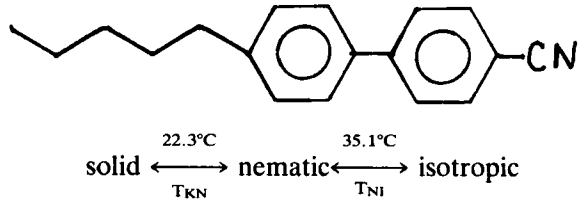

The cell geometry for our transverse-field observation is shown in Figure 1. The cell consists of a nematic liquid crystalline layer sandwiched between two glass

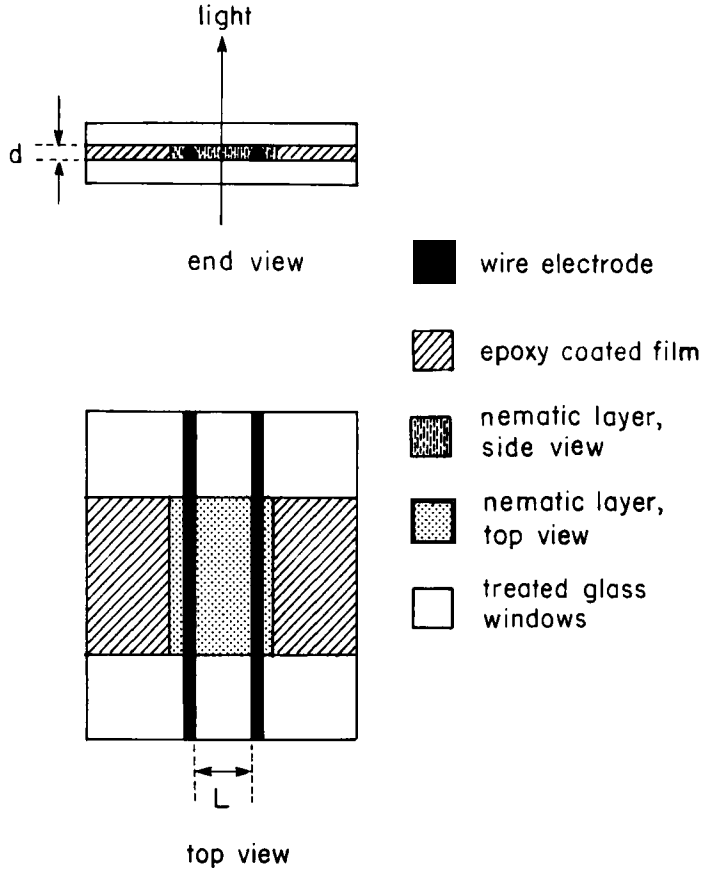

FIGURE 1 Geometry of a "thick"-electrode cell.

plates. The glass plates were chemically cleaned and treated with dichlorodimethyl silane to produce spontaneous, homeotropic alignment of the nematic molecules perpendicular to the glass. The plate separation, d, was varied from 2.5 to 42 microns and measured interferometrically. An electric field is applied across the nematic layer by means of two electrodes. The electrodes may be as thick as d ("thick"-electrodes) or much thinner ("thin"-electrodes). The "thick"-electrode construction uses fine diameter wire as the electrodes; whereas, the "thin"-electrode construction uses thin films (about 1 micron) of conducting indium oxide. The electrode separation, L, was varied between 1 and 4 mm. Because the field is perpendicular to the direction of light through the cell (see Figure 1), the assembly is called a transverse-field cell.[8]

Optical observations of the field-induced deformation structures were made using a Zeiss polarizing microscope at low magnification (typically 30X).

OBSERVATIONS

Without field, the nematic between the two electrodes appears black in cross-polarized light. This condition remains when the sample stage is rotated through 360°. When conoscopic light is used, the interference pattern shows an optically-centered cross. This indicates the molecules are perpendicular to the glass surface.

When an AC voltage is applied, colorful birefringent patterns are produced. Figure 2 shows a typical series of patterns produced by applying a 60 Hz AC signal across a cell with an $L = 2.2$mm and $d = 12.4$ microns. The observations made in cross-polarized light are summarized below.

The inter-electrode area is entirely dark until a threshold field, E_c, is reached. At this field, birefringence is first perceptible at both electrodes. As the field strength is increased further, the birefringent regions near both electrodes increase, forming a symmetrical pattern (Figure 2a). A series of colored bands, indicating the degree of molecular reorientation, exists between the linear interface and the electrode. At a field for wave-onset, E_w, perturbations in the linear interfaces are just perceptible (see Figure 2b). Above E_w, the amplitude of the perturbations increases and a regular wave pattern is developed (Figure 2c). The wavelength, λ, depends on the cell thickness and temperature. Eventually, the birefringent regions emanating from either electrode merge in the center of the inter-electrode region (Figure 2d). When this occurs, the wave structure collapses. This can be accompanied by a complete coalescence of the advancing birefringent regions; or a black disclination line may remain, dividing the two regions. These observations are reversed upon reducing the field strength.

RESULTS

The effect of layer thickness on the wavelength of the wave structure is shown in Figure 3. The values reported were measured at 22°C using a 140 volt, 60 Hz AC signal. The data are plotted versus reciprocal thickness to emphasize the limiting

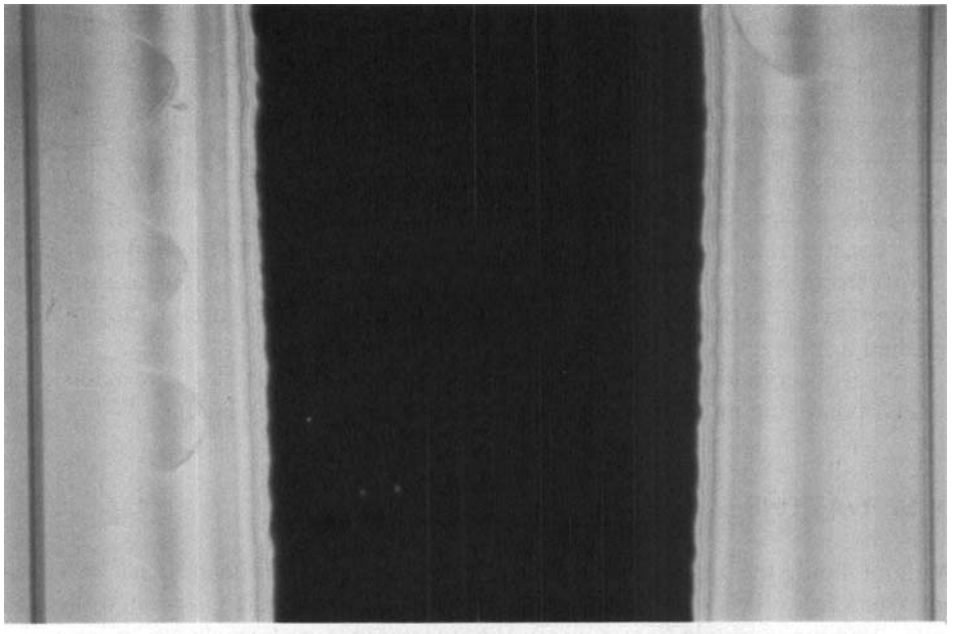

(a)

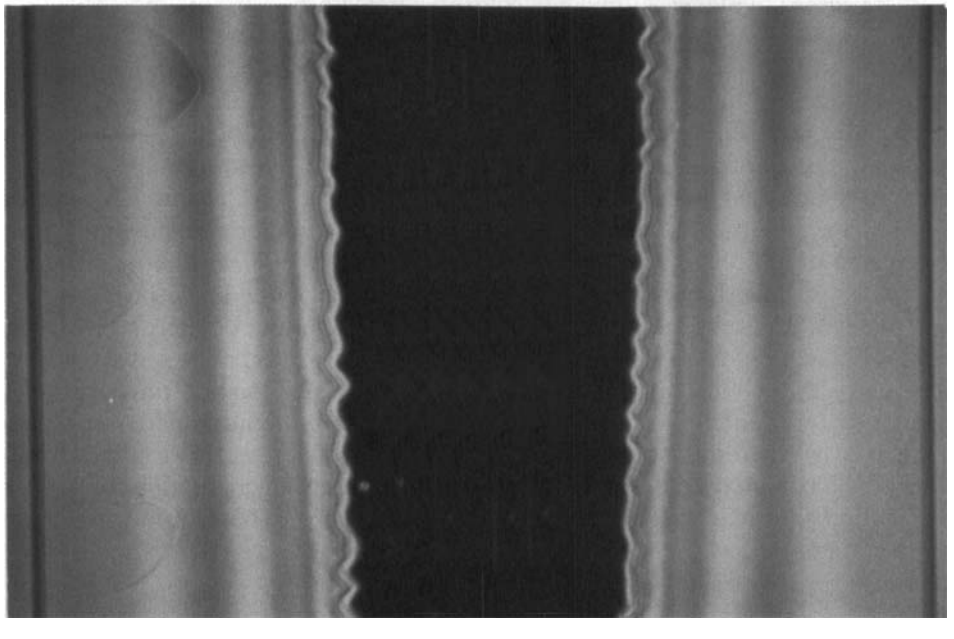

(b)

FIGURE 2 60 Hz AC deformation patterns for a "thick"-electrode cell with $L \approx 2.2$ mm and $d = 12.4$ microns. Field strengths are: a) 900 V/cm, b) 1100 V/cm (E_w), c) 1250 V/cm and d) 1450 V/cm. See Color Plate I.

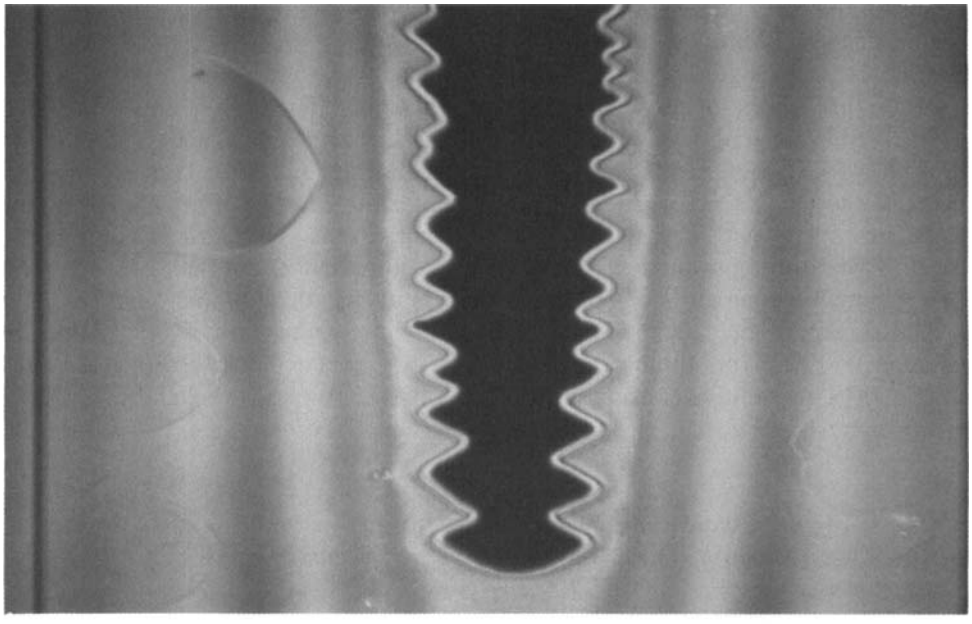

(c)

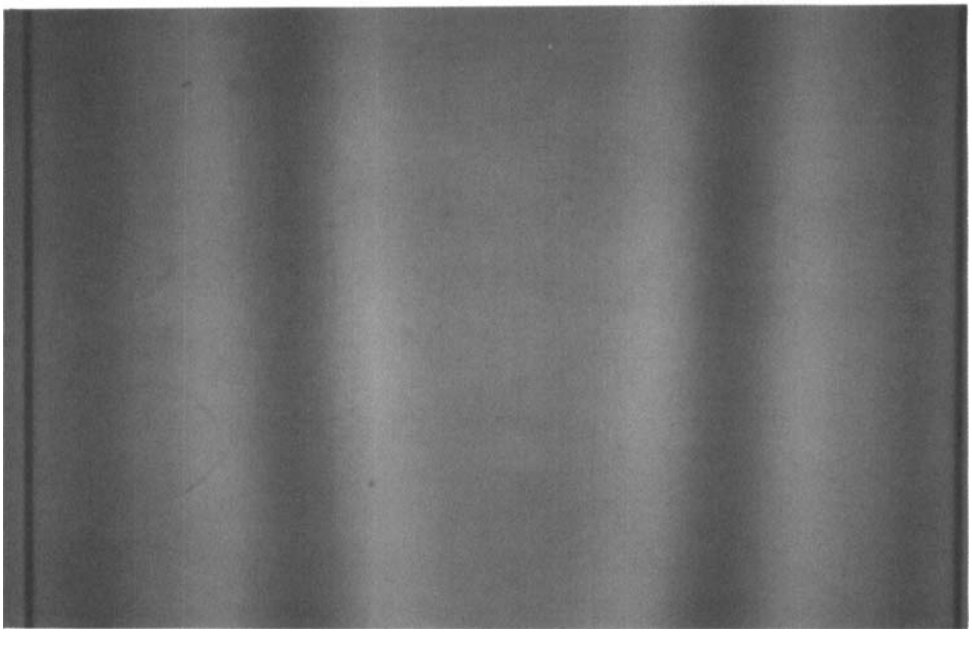

(d)

See Color Plate II.

effects of the glass surfaces on thick and thin layers. From this figure, two thickness regimes can be identified. Layers thinner than about 10 microns ($1/d > 0.1$) have a constant wavelength of about 20 microns. For thicker layers, the wavelength of the structure scales linearly with reciprocal thickness. The y-intercept of this line predicts the wavelength of an infinitely thick layer to be 330 microns. Experimentally, however, waves could not be established in layers thicker than 42 microns because the two interfaces merged in the center of the cell before wave forming conditions were met. These results suggest that: 1) the glass surface plays a stabilizing role in the production of the wave structure and 2) the bulk properties of the nematic become more important for layers thicker than 10 microns.

The threshold field dependence, E_c, also demonstrates two regime behavior (Figure 3). For layers thinner than 10 microns, E_c scales linearly with reciprocal thickness. This trend is expected. Soref[8] predicts E_c to obey the equation:

$$E_c = (\pi/d)\,(K_{33}/\Delta\epsilon\epsilon_o)^{1/2} \tag{1}$$

where K_{33} is the elastic constant for bend deformation and ϵ_o is the permittivity constant for a vacuum. Thus, from the slope of our curve, we calculate K_{33} to be

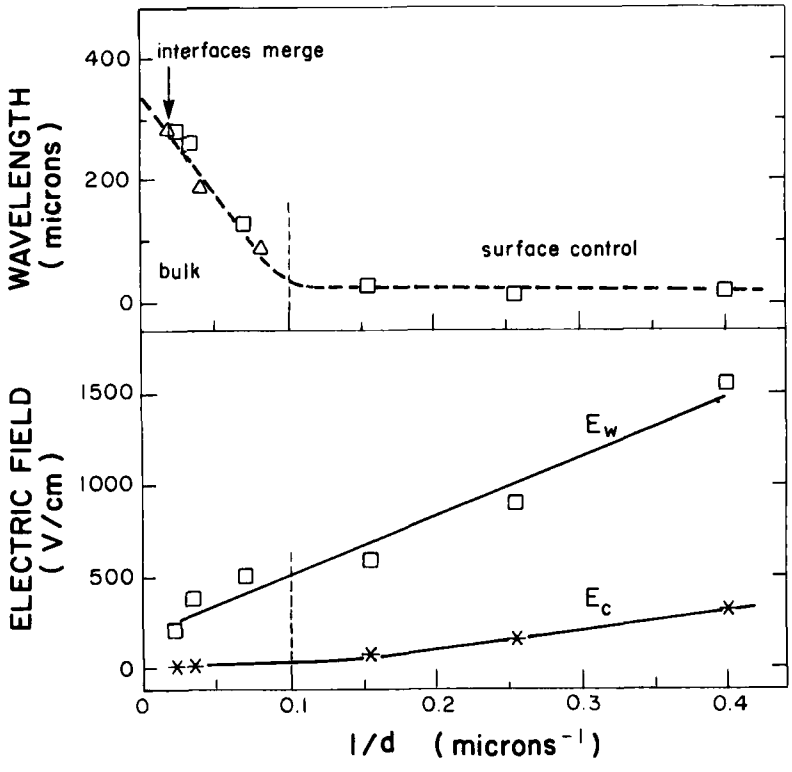

FIGURE 3 Wavelength, wave-onset field, E_w, and threshold field, E_c, plotted versus reciprocal thickness.

9.1×10^{-6} dynes. This is within a decade of the value of 1.69×10^{-6} dynes reported for the same compound by Karat and Madhusudana.[9] For thicker layers, E_c is small (of the order of 10 V/cm).

The wave onset field, E_w, was found to scale linearly with reciprocal thickness as shown in Figure 3.

The temperature dependence of the wave structure at a constant applied voltage is shown in Figure 4. "Thick"- and "thin"-electrode configurations gave equivalent results. The wavelength of the waves increased linearly with temperature from 22 to 32°C. Concomitantly, the definition of the wave structure became more diffuse with increasing temperature. From 32 to 35°C, the wave structure destabilized entirely and the interface became linear. These results will be discussed in the following section. Above the clearing point (35°C), no birefringence and no wave structures were observed as expected.

The interface position may be quantified by a dimensionless number, x/L, where x is the distance from the electrode to the interface. Values range from 0 (for $E < E_c$) to 0.5, where the two interfaces merge in the center of the cell. For reasons

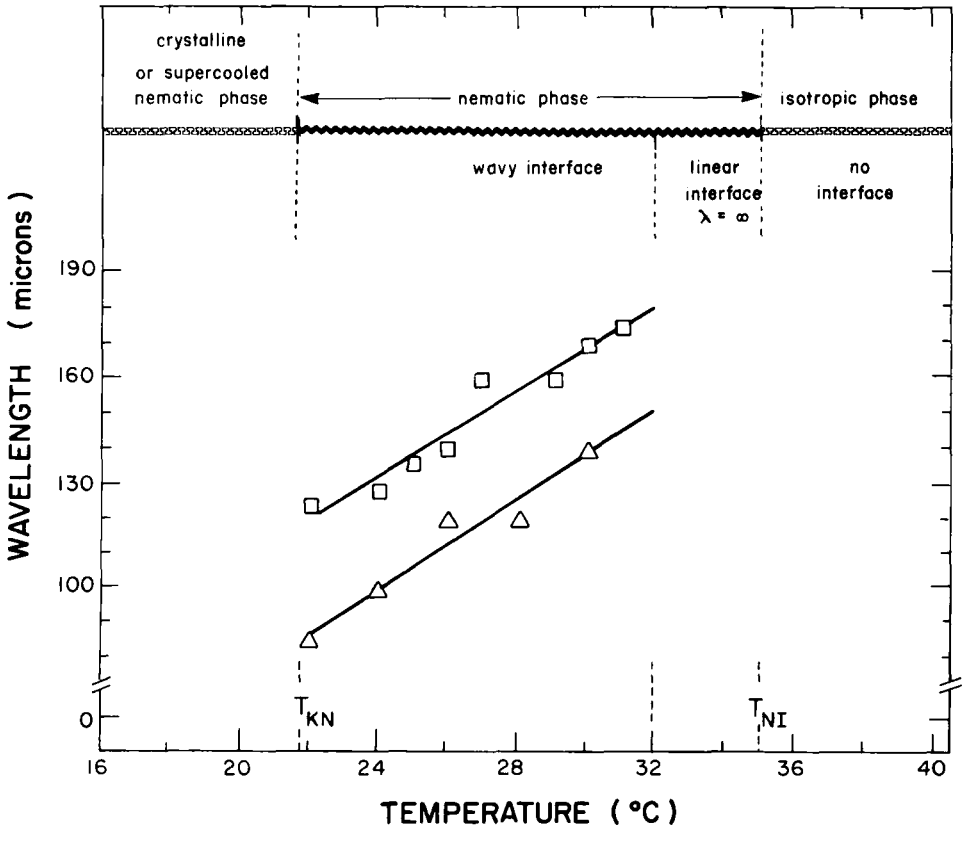

FIGURE 4 Temperature dependence of wave structure for cells of two electrode geometries: □—14 micron, "thick"-electrode cell; △—12 micron, "thin"-electrode cell.

which will become apparent later, the square-root of this quantity is plotted versus electric field for a series of "thin"-electrode cells in Figure 5. The interface is linear at low fields, and wavy at high fields. The wave onset field, E_w, is encircled. As the field is increased above this level, the amplitude and definition of the waves increase. Typically, waves occur closer to the center for thicker layers.

Figure 5 also shows a linear relationship between $\sqrt{x/L}$ and E. Since L is identical for these cells and $V = EL$, it follows that x/L scales linearly with V^2. The equation for energy storage as a function of time, $W(t)$, in a parallel plate capacitor is given by:

$$W(t) = CV^2(t)/2 \tag{2}$$

where C is the capacitance of the cell driven by the time dependent voltage $V(t)$. Thus, an analogy is made between the interface position and the electrical work done on the nematic. Deviations from linearity in the initial regions of the $\sqrt{x/L}$ vs E curves can be either positive or negative. For thin samples, where the initial deformation is dominated by the surface and E_c was found to be large, the deviations

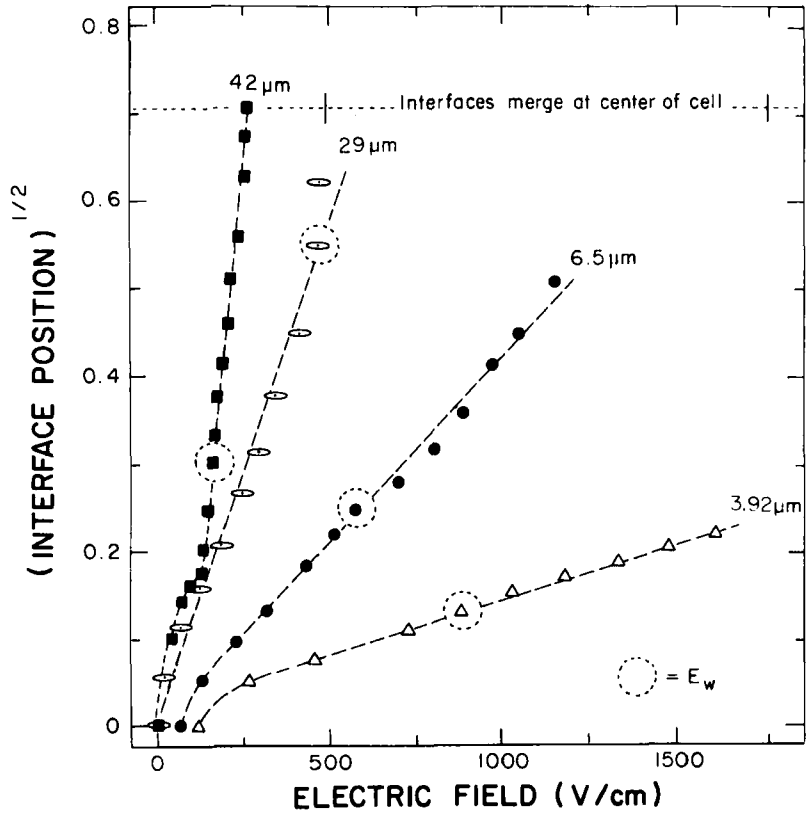

FIGURE 5 Square root of interface position versus electric field for a series of "thin"-electrode cells.

are negative. For thick samples, where bulk properties become more important and E_c was found to be small, the deviations are positive.

The conditions of temperature and frequency which stabilize the wave structure are shown in Figure 6. The data span a frequency range from 200 to 2000 Hz at constant voltage and cover the entire nematic temperature range. This figure shows that high frequencies and low temperatures promote the formation of the wave structure. These are conditions where the nematic mesophase responds to a deformation more like an elastic solid than a viscous liquid. The definition of the wave pattern also sharpens under these conditions.

DISCUSSION

The birefringent patterns shown in Figure 2 are the result of electrically induced torques acting on the nematic. The origin of these torques can be either ionic or dielectric in nature. Defining the space-charge relaxation frequency[8], f_c, as

$$f_c = \sigma_\perp / 2\pi\epsilon_\perp \epsilon_o \tag{3}$$

where $\sigma_\perp$ and $\epsilon_\perp$ are the perpendicular components of the anisotropic conductivity and permittivity, respectively, two regimes can be identified. For $f < f_c$, the cell

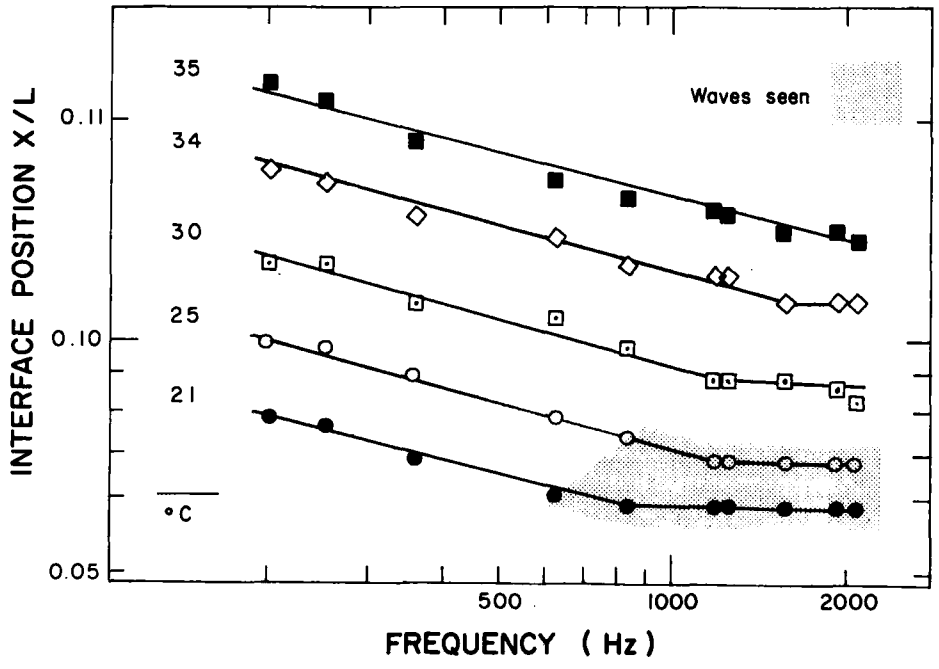

FIGURE 6 Interface position versus frequency for a cell with d = 14 microns, L = 1.98 mm and E = 700 V/cm.

operates in the conductive regime: for $f > f_c$, the cell operates in the dielectric regime. In the conductive regime, ionic impurities, injected charges or ions formed by dissociative processes have ample time to migrate during one-half cycle of the voltage. Thus, orientation caused by shear-induced torques are possible. In this regime a frequency dependent interface position is expected. In the dielectric regime, ionic motion is limited and orientation caused by dielectric torques predominate. Here, a frequency independent interface position is expected (in contrast to the threshold field dependency). This suggests that the frequency independent region of the curves in Figure 6 correspond to the dielectric regime and the negatively sloped linear portions correspond to the conduction regime.

For 4-4′-*n*-pentylcyanobiphenyl at 21°C[10], we calculate f_c to be about 240 Hz. From the equivalent temperature curve of Figure 6, the wave structure is observed above 625 Hz. Thus, the wave structure occurs in the dielectric regime. The absence of dust particle motion at the wave-like interface supports this conclusion since it rules out ionic flow.

Because the regular wave pattern produced here is similar to the schematic pattern shown in the paper by Helfrich,[11] we believe the wave structure is the result of space-charge build-up.[11,12] As the nematic reorients, the dielectric constant of the liquid increases ($\epsilon_\parallel \approx 15$, $\epsilon_\perp \approx 6$). This increases the charge storing capacity of the liquid and allows the field to penetrate further.

At $f > f_c$, charges can accumulate locally,[11] disrupting the homogeneity of the dielectric field. According to the theory,[11] as simplified by deGennes,[13] an instability in the orientation pattern can occur when the dimensionless parameter δ^2 is greater than unity. This parameter is given by

$$\delta^2 = \left(1 - \frac{\sigma_\perp}{\sigma_\parallel}\frac{\epsilon_\parallel}{\epsilon_\perp}\right)\left(1 + \frac{\alpha_2 \epsilon_\parallel}{\eta_c \Delta\epsilon}\right) \tag{4}$$

where α^2 and η_c are viscosity coefficients and the other parameters have been defined previously. Substituting the viscosity values of MBBA[14] for our sample, we calculate[10] δ^2 to be 33.5 at 21°C and 1000Hz. Thus, the wave instability is predicted from theory and confirmed experimentally (see Figure 6). The temperature dependence of δ^2 is non-trivial because all six of the material parameters in Equation 4 are temperature dependent. However, these parameters vary slowly for temperatures well below the nematic-isotropic transition. Thus, we expect the wave instability criterion, δ^2, to continue to be met in this temperature region. This is confirmed from Figure 4 where a wavelength can be measured between 22 and 32°C. As the nematic-isotropic transition is approached to within 3 or 4 degrees, the material parameters vary more rapidly and change in such as manner as to lower δ^2 below unity. Here, no wave pattern is established and the interface becomes linear (see Figure 4). As for the temperature dependence of the wavelength, we speculate this depends critically on the elastic constants of the sample. The loss of sharpness in the wave-like interface with temperature is attributed to increased thermal fluctuations.

At $f < f_c$, destabilization of the wave structure occurs. In this regime, conduction

currents are allowed to flow. These currents neutralize the space-charges thus destroying the wave structure.

CONCLUSIONS

Orientation patterns caused by the action of an electrical field on a mono-domain nematic liquid crystal are varied and interesting. This paper describes an interesting wave structure observed in thin nematic layers for a particular electrode geometry. The regular wave structure occurs in the dielectric regime of an electrical deformation and is believed to be the result of space-charge build-up.

Acknowledgments

The authors would like to thank Robert Meyer at Brandeis University and George Durand at CNRS (Orsay) for their encouragement and helpful discussions.

References

1. G. H. Heilmeier, L. A. Zanoi and L. A. Barton, *Proc. IEEE*, **56**, 1162 (1968).
2. W. W. Hollaway, Jr. and M. J. Rafuse, *J. Appl. Phys.*, **42**, 5395 (1971).
3. M. J. Schiekel and K. Fahrenschon, *Appl. Phys. Lett.*, **19**, 391 (1971).
4. W. Haas, J. Adams and J. B. Flannery, *Phys. Rev. Lett.*, **25**, 1326 (1970).
5. F. J. Kahn, *Appl. Phys. Lett.*, **20**, 199 (1972).
6. I. G. Chistyakov and L. K. Vistin, *Kristallografiya*, **19**, 195 (1974).
7. A. P. Kapustin and L. S. Larinova, *Kristallografiya*, **9**, 297 (1963).
8. R. A. Soref, *Appl. Phys. Lett.*, **22**, 165 (1973).
9. P. P. Karat and N. V. Madhusudana, *Mol. Cryst. Liq. Cryst.*, **40**, 239 (1977).
10. $\sigma_\perp = 0.83 \times 10^{-10}$ nS/cm, $\sigma_\parallel = 0.13 \times 10^{-10}$ nS/cm, $\epsilon_\perp = 6.0$, $\epsilon_\parallel = 15.3$. All measurements taken at 21°C and 1000Hz.
11. W. Helfrich, *J. Chem. Phys.*, **51**, 4092 (1969).
12. E. Dubois-Violette, P. G. deGennes and O. Parodi, *J. Physique*, **32**, 305 (1971).
13. P. G. DeGennes, *The Physics of Liquid Crystals*, Oxford Press University, Oxford, 1974.
14. $\alpha_2 = -77.5$ poise, $\eta_c = 41.6$ poise; from Reference 13.